Natural gas engines modeling: combustion and NOx emissions prediction

Main authors

Guillaume Peureux, Olivier Baudrand, Ghislain Lartigue, Stéphane Carpentier, Carole Etienne

GDF SUEZ, Direction de la Recherche et de l'Innovation, 361 av. du Président Wilson, B.P. 33, 93211 Saint-Denis La Plaine cedex, France

1. ABSTRACT

Nowadays there are 7,1 million Natural Gas Vehicles (NGV) in operation all around the world. Recognized as the cleanest hydrocarbon fuel, Compressed Natural Gas (CNG) enables a 23% reduction in CO_2 emissions from combustion in the engine, compared to the gasoline reference. This alternative fuel is fully compatible with the biomethane use (produced from a wide range of bio-wastes and raw biomass). In addition, today oil prices make CNG with its current low cost an even more interesting alternative fuel.
However, the need to secure supplies of natural gas may lead to an increasing risk of variation of its composition / quality at the delivery point. Thus, its properties as a fuel have not been mastered by the cars and trucks industries yet. In order to support manufacturers to optimize their natural gas engines, GDF SUEZ has developed a simulation tool based on its expertise over natural gas combustion to predict the impact of natural gas composition on power output and exhaust emissions. Its purpose is twofold: (i) to analyze the influence of gas quality on the engine behavior, (ii) to support the development of engine control strategies to keep a constant power output (with a driving feeling comparable to a commercial gasoline vehicle) and satisfactory exhaust emissions (with respect to current and future pollution standards) over a wide range of natural gas compositions.

The objective of this study is, on one hand to implement a satisfactory NO emission model in the former homemade engine simulation code and so to reinforce its prediction abilities and, on the other hand, to implement natural gas issues into an industrial simulation platform well spread over the car industry. These results will then be used in collaborative research programs to strengthen interactions with car manufacturers and to take a better hold on the NGV market development. The results of the first part of the study led to the choice of a NO emission model with a narrow error interval, giving good confidence in respect to emission tendencies throughout the engine operation conditions. The second part of the study led to a specific library for natural gas used as a fuel in LMS Imagine.Lab AMESim® software, that can be used with IFP-Engine® library. The quality of the estimation results over experimental data was similar to the ones obtained with IFP-Engine® used for gasoline operation simulation under the same conditions. Few parameters that remained as default values in this study will be tuned in the future to get even more satisfactory results, which will be compared to gasoline simulation performances with fitted parameters.

C O N T E N T S

2. INTRODUCTION

In nowadays' energy context with high oil prices, Compressed Natural Gas (CNG) appears to be a cheap alternative fuel, more sustainable (longer-term fossil resources than oil) and compatible with the biomethane use (produced from a wide range of bio-wastes and raw biomass). Vehicles fuelled and powered by CNG have less impact on the environment (23% reduction in CO_2 emissions in comparison to gasoline and lower local pollutants emissions). Finally, natural gas supply and markets suffer less than the oil supply and markets as natural gas resources are well spread over the world and located in safe and stable areas.

As natural gas is distributed to end-customers through an international interconnected network, with various injection ports all along the gas grid and different origins of supply, its composition may vary all along the grid and over the time. The need for a security of supply requires various sources of natural gas which could lead to an increasing risk of variation of its composition / quality at the delivery point.

Fluctuations in fuel composition may particularly affect the combustion quality at lean operating limit conditions. Thus, the stability of fuel specifications is an important parameter for engine manufacturers to achieve the best compromise between high level of power, low consumption, low emissions and the knock prevention.

Cars and trucks manufacturers are not experts in natural gas, and bringing them further skills is a condition to the success of the NGV market development. In order to help to optimize their CNG engines, GDF SUEZ has developed a simulation tool based on its experience of natural gas combustion to predict the impact of natural gas composition on power output and exhaust emissions. Its purpose is to analyze the influence of gas quality on the engine behavior, and how throttling, spark timing, air / fuel ratio or recirculation of burnt gases can help, keeping a constant power output (with a constant driving feeling, comparable to a commercial gasoline vehicle) and satisfactory exhaust emissions (with respect to current and future pollution standards) over a wide range of natural gas compositions.

This tool is a time-scaled 0 dimensional calculation code which was first written in Fortran 90 [1]. The combustion part consists in a two-zone thermodynamic model. Flow description and thermodynamics are calculated thanks to usual models for 0 dimensional codes [2], with a high focus on the impact of quality variations of natural gas as a multi component gaseous fuel.

Today, this former Fortran 90 homemade model has been implemented in an industrial platform well spread over the car industry: LMS Imagine.Lab AMESim®. The objective is then to use this tool in collaborative research programs to strengthen interactions with car manufacturers and to take a better hold on the NGV market development.

3. EXPERIMENTAL FACILITIES

Engine tests have been conducted on a light-duty spark ignition engine designed for both gasoline and CNG operations. This engine has a capacity of 1.4 liter with a volumetric compression ratio of 10:1.

The test rig main characteristics are: maximum torque of 1,400 Nm, maximum rotational speed of 8,000 rpm, maximum power of 255 kW (345 hp).

Natural gas composition is adjusted with a proprietary in-line gas mixer. Flow is measured with a Coriolis mass flow meter. Dedicated mass-flow meters control adjunctions of pure nitrogen, ethane, propane and butane into base pure methane fuel. This system enables the synthesis of a wide range of natural gas compositions with a restricted number of gas cylinders. As a

consequence, this process can significantly reduce the cost of the fuelled gases, compared to premixed compositions.

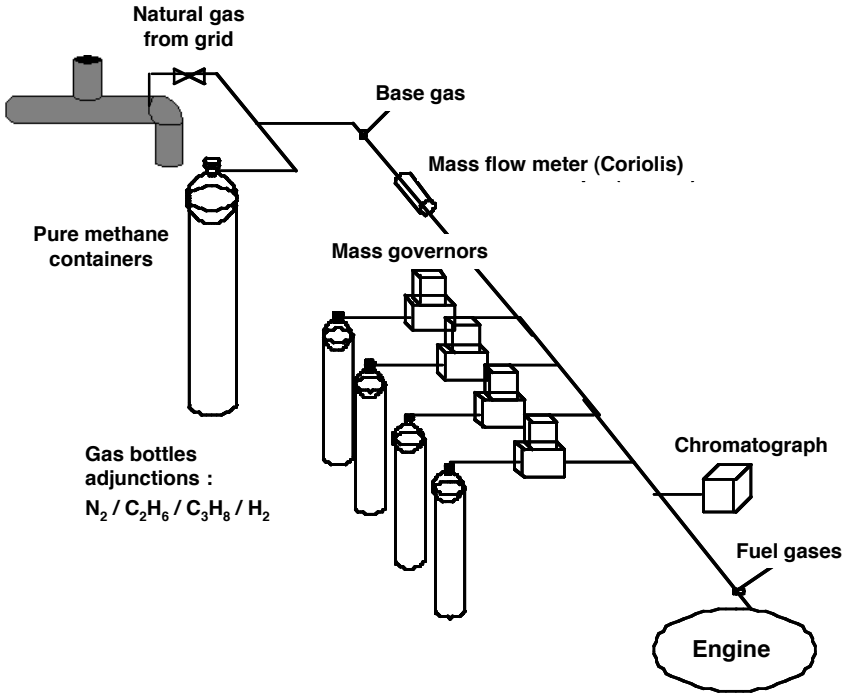

Figure 1: Test rig in-line mixer overview

This test bench enables accurate synthesis of five pure gas mixtures (including methane) and also the injection of a liquid fuel (such as butane) into the blend.

Combustion products NO_x, C_nH_m, O_2, CO, CO_2, CH_4 are measured. An online chromatograph is used to check fuelled natural gas composition before each test. Instantaneous cylinder pressure, inlet and outlet gases temperatures, inlet and outlet cooling water temperatures, static pressure in the intake manifold and various other parameters are also measured.

Engine tests have included more than a thousand different points with variations in natural gas composition, load, fuel-air equivalence ratio, spark timing and engine speed.

An average natural gas composition was initially chosen, and the other natural gas compositions were obtained by addition, either separately or jointly, of ethane, propane, butane, nitrogen and hydrogen. Hydrogen was also used for tests with Hythane® composition: 20% of hydrogen in volume with 80% of natural gas.

4. NOX EMISSIONS MODELING

The present study focuses on the development of a NO post-processor coupled with the natural gas engine simulation tool [1].

4.1. Description of the NO model

The NO model implemented in the post-processor is based on the well-known Zeldovich mechanism, with constants available from the literature [3,4].

This NO mechanism consists in the following reactions [5-12]:

$$O + N_2 \leftrightarrow NO + N \quad (1)$$
$$N + O_2 \leftrightarrow NO + O \quad (2)$$
$$N + OH \leftrightarrow NO + H \quad (3)$$

These reactions constants can be written in the following form:

$$K = A \cdot T^B \cdot e^{-\frac{E}{R \cdot T}}$$

Formation constants are usually quoted K^+ (forward direction) and dissociation constants K^- (backward direction). A, B and E constant values are gathered in Table 1.

	K^+			**K^-**		
Reaction	**A (cm^3/mol.s)**	**B(-)**	**E (J/mol)**	**A (cm3/mol.s)**	**B (-)**	**E (J/mol)**
1	$1{,}36.10^{14}$	0	315900	$3{,}27.10^{12}$	0,3	0
2	$6{,}4.10^{9}$	1	26300	$1{,}5.10^{9}$	1	162100
3	$6{,}8.10^{13}$	0	0	$2{,}0.10^{14}$	0	196600

Table 1: Formation and dissociation constants for NO mechanism: [3,4]

For each of these reactions, R_i is the reaction rate at the equilibrium of reaction (i):

$$R_1 = K_1^+ \cdot [N_2]_e \cdot [O]_e = K_1^- \cdot [NO]_e \cdot [N]_e$$
$$R_2 = K_2^+ \cdot [O_2]_e \cdot [N]_e = K_2^- \cdot [NO]_e \cdot [O]_e$$
$$R_3 = K_3^+ \cdot [OH]_e \cdot [N]_e = K_3^- \cdot [NO]_e \cdot [H]_e$$

With:

- K_i : reaction kinetic constant of reaction (i) (cm^3/mol.s),
- $[X]_e$: concentration at equilibrium of species X (mol/cm^3),
- R_i : reaction rate at equilibrium for reaction (i) (mol/cm^3.s).

Among the species involved in these reactions, Kesgin [5] states that part of them can be regarded close to equilibrium since they are reactants of other combustion reactions which are much faster than (1), (2) and (3): O, O_2, OH et H. Only NO and N cannot be considered close to equilibrium. Choosing α and β variables as follows,

$$\alpha = \frac{[NO]}{[NO]_e} \text{ and } \beta = \frac{[N]}{[N]_e}$$

and following Kesgin [5], NO and N formation rates are written here as a function of time:

$$\frac{d[NO]}{dt} = R1 + \beta(R2 + R3) - \alpha(\beta R1 + R2 + R3)$$
$$\frac{d[N]}{dt} = R1 + \alpha(R2 + R3) - \beta(\alpha R1 + R2 + R3)$$

Considering quasi-steady state hypothesis for N, the NO formation rate is then written:

$$\frac{d[NO]}{dt} = \frac{2 \cdot R_1 \cdot (1 - \alpha^2)}{(\alpha \cdot \frac{R_1}{R_2 + R_3} + 1)}$$

In this study, the mass of burnt gases created during each time step of combustion calculation is stored and considered as a burnt gas zone. The temperature and pressure in this zone evolve under the same conditions as the rest of the burnt gases.

We have considered here that there is no transfer of matter between the burnt zones created. As shown on Figure 2, for a given time step and a given burnt zone, the initialization value used for NO formation evolution is the NO previously formed in this zone for the existing burnt zones and is zero for the currently burning zone. Each zone has an independent evolution.

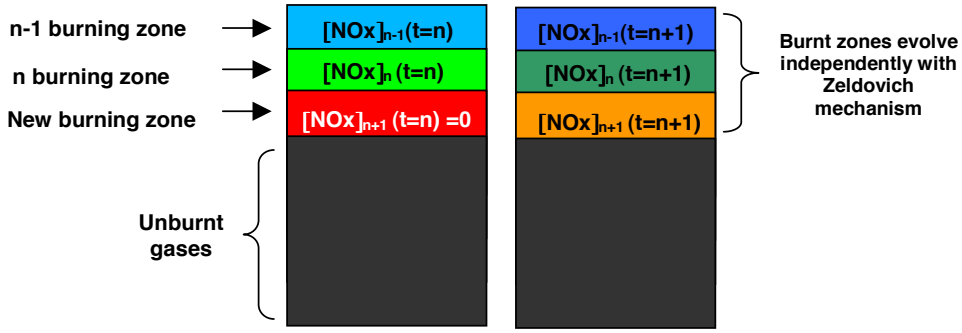

Figure 2: Evolution of NO concentration at a given time step in the burning zone and exhaust gases

4.2. NO model results

Among NOx emissions out of the engine, NO emissions account for a high proportion of these. The same modeling is to be done with NO_2 to increase accuracy. Before testing various NOx models, calibration of combustion parameters in the engine combustion code has been achieved carefully.

Regarding the combustion model, previous works were dedicated to laminar flame speed calculations for natural gas mixtures over temperature and pressure ranges for which experimental data are not easily available. A calibration of a turbulent constant in the combustion model and the delay between the spark ignition and the start of combustion led to good estimations of in-cylinder pressure evolution which is the most influenced quantity by variations in the combustion process. The chosen parameters for calibration were: cycle maximum pressure level, crank timing over the cycle and indicated mean effective pressure.

Since instantaneous pressure data in the intake manifold were not available, a residual burnt gases rate was calibrated over 20% of all experimental data in order to get better accuracy over in-cylinder mixture mass during closed valve phases in the engine cycle. Dependency over load and engine speed was then taken into account to create a formula describing the evolution of this residual burnt gases rate over experimental data. In-cylinder mass has been determined with this formula.

Due to a lack of data on wall temperature of the engine, thermal losses were put as default values without introducing dependency over load. Thus, evaluation of the NO model has been focused on error distribution over the simulated points, rather than on error itself.

NO calculations were then obtained on more than 130 experimental points. Results showed that NO emissions were underestimated. The main reason would be an overestimation of thermal losses due to too high default values for thermal exchange constant in the dedicated correlation from Hohenberg [13], and the need to introduce a dependency between wall temperature and load variations. Despite the lack of accuracy due to overpredicted thermal losses, the ability of the model to give satisfactory tendencies predictions can be examined through these results: mean error is 27.3%, while 80% of errors are included between 20.7% and 32.9%.

The model gives satisfactory error distribution with a quite narrow interval.

As NO production is quite sensitive to temperature level in the burnt gas zone, predictions of NO emissions tendencies over all the simulated points give another confirmation on the relevance of the calculated temperature for burnt gases, and so the whole combustion model used.

As a matter of fact, calculations that were done to see the influence of a 5% decrease in burnt gases temperature resulted in a decrease in NOx estimation by around 50%.

The kinetic constants that have been used in this study are exactly those given in [3,4] (see Table 1): no particular tuning has been performed to achieve the results. However, when all the combustion parameters will have been calibrated, and if discrepancies between experimental data and numerical results still arise, we will eventually modify these constants to enhance our NO model prediction.

Figure 3 shows emissions predictions over tests at full load with engine speed variations with two different natural gases compositions listed in Table 2.

	NG1	NG2
CH_4	82.8	82.3
C_2H_6	10.5	5.0
C_3H_8	3.8	1.8
C_4H_{10}	2.0	0.0
N_2	0.9	10.9

Table 2: Example of 2 natural gas compositions tested

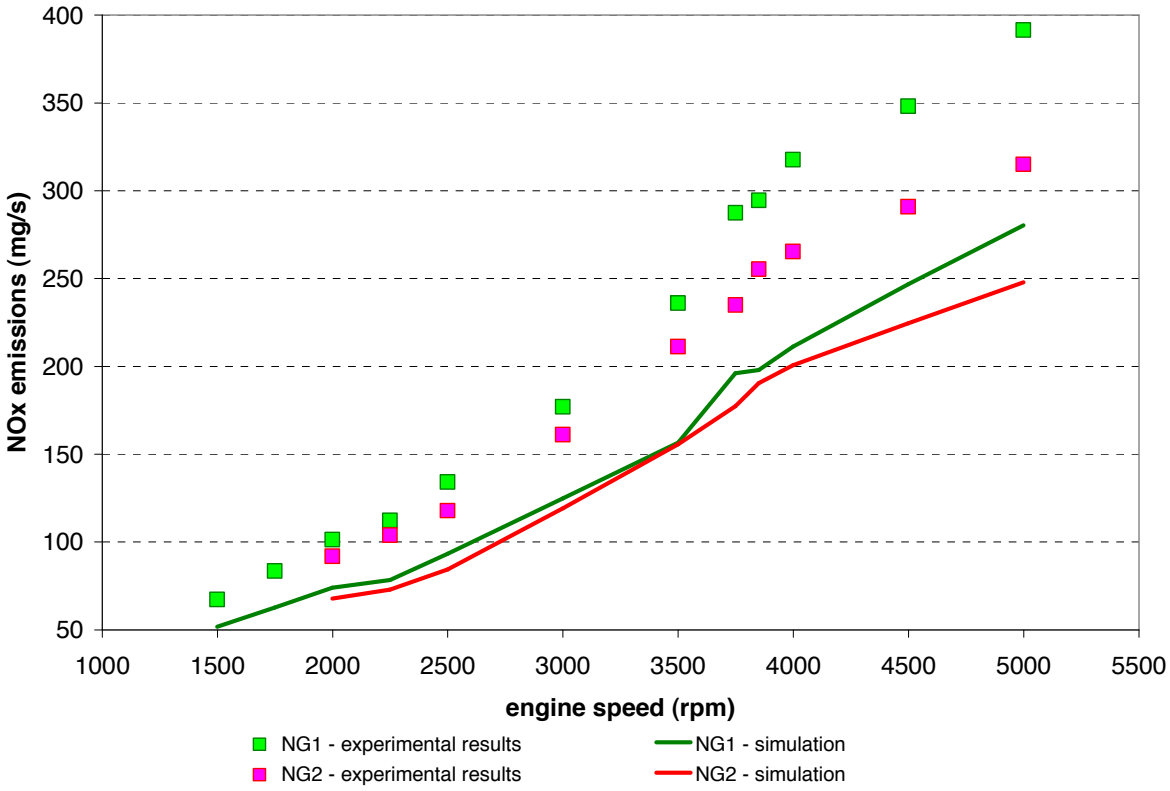

Figure 3: NOx emissions at full load with engine speed variations (experimental data and simulations) for two natural gas compositions

Tendencies in NO formation are well predicted over the simulated points, with respect to engine speed and gas quality variations.

Higher accuracy in the NO prediction may be achieved through thermal loss calibration and introducing a dependency between wall temperature and load variations.

5. IMPLEMENTATION OF NATURAL GAS AS A FUEL IN AN INDUSTRIAL SIMULATION TOOL

This study has been achieved in parallel with the previously presented NOx modeling study. Its objective was to implement GDF SUEZ homemade engine simulation model into the well spread simulation tool LMS Imagine.Lab AMESim®. A short review of the IFP-Engine® library showed many common points between the two engine combustion models and pointed out which parts of the CFM-1D model developed by IFP [14] could be adapted in order to take into account natural gas characteristics as a fuel. The implementation then resulted in a dedicated CNG library which is used in combination with the IFP-Engine® library.

Focus has mainly been put on the introduction of natural gas composition in the fuel definition, thermodynamic properties calculations, and laminar flame speed calculations with dependency over equivalence ratio, residual and EGR (Exhaust Gas Recirculation) rate and the composition of natural gas with methane, ethane, propane, butane, nitrogen and carbon dioxide. Hydrogen has also been added for Hythane® simulations.

The natural gas library has then been used to simulate the behavior of the tested engine.

5.1. Calibration method for the combustion model in this study

For these very first calibrations of the combustion model on the AMESim® platform, closed valve calculations have been performed. The main parameter that has been fitted in this study is the tumble constant of the model. Other parameters have been kept to the software's default values: C_{dis} and C_{turb} that control turbulence creation and destruction phasing along the cycle, and the model for realistic wrinkling of flame that controls turbulence description of the early combustion phase. Wall temperature has been kept constant to an arbitrarily chosen value over all the simulated engine tests because of lack of data. Dependency between this temperature and load will have to be introduced to achieve more accurate results.

Calibration of the model has been done over 20% of all experimental data, so that the prediction ability of the model could have been tested over a large panel of experimental data without the model's calibration on them.

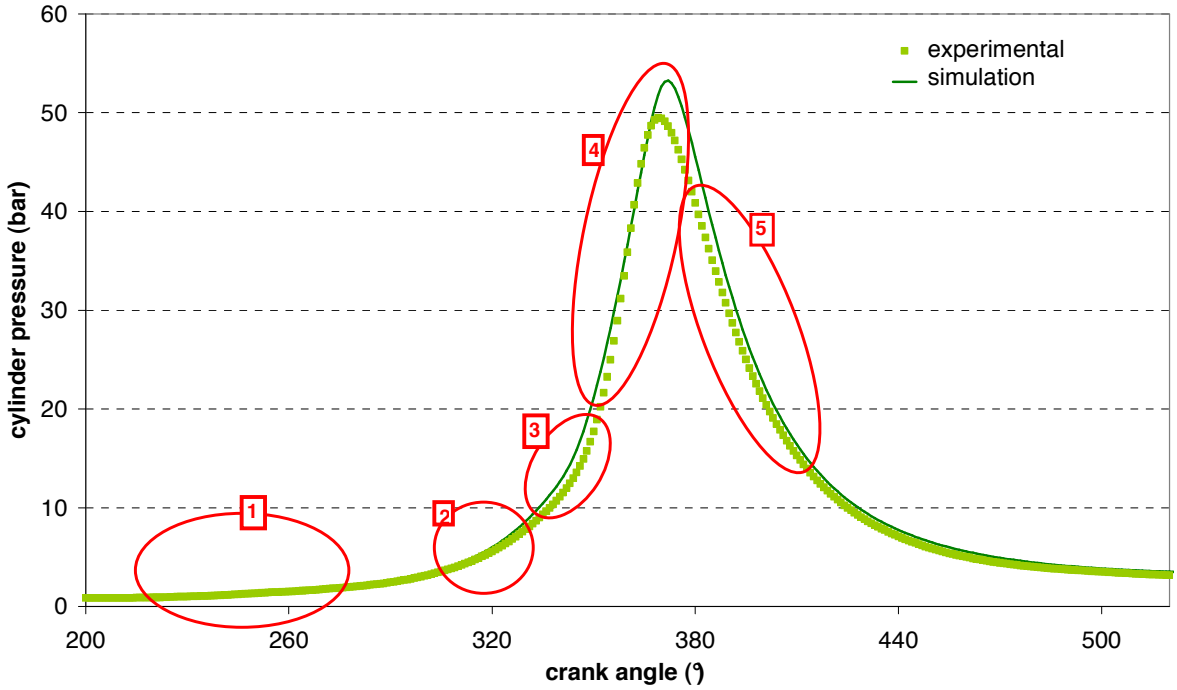

Figure 4: Cylinder pressure: comparison between experimental data and simulation result - simulation key parameters to reproduce experimental behavior

Figure 4 shows a comparison between cylinder curves from test and simulation results. The various steps for CFM-1D model calibration that are highlighted in the graph are:

1. In cylinder mass:

Mass calibration is achieved through residual gases rate estimation. In this study, after a calibration for each tested point, a correlation has been determined and used for all following model calibration steps. It does not take into account some particularities of each point such as exhaust temperature, or acoustic waves magnitude.

2. Start of compression phase:

At this step, thermal losses for compression phase have to be calibrated. Error in pressure estimation can be induced here by in cylinder mass estimation error, and then, also by:

- Compression ratio uncertainty due to manufacturer's production tolerance,
- Thermal losses, because the calibration is averaged over all experimental data from the tests,
- Ideal gases hypothesis may not be representative of real behavior.

3. Start of combustion:

Initial flame volume parameter has to be calibrated. In this study, after a calibration calculation for all points, one chosen value was then used for all following calibration steps. When using the model for realistic wrinkling of flame, relevance and method of this parameter's calibration will have to be examined.

4. Tumble:

Calibrations have been done for the tumble parameter at the same time as calibrations of start of combustion phase, and thermal losses at expansion phase so as to choose relevant values for these parameters. Final calibration of the tumble parameter has been done when all other calibrations are made.

5. Expansion phase:

Thermal losses have also been calibrated at expansion phase. During this phase, all cumulated errors are gathered. Same reasons as for compression phase may explain specific errors (not induced by previous calibrations) in this phase.

5.2. Residual gases rate calibration

With lack of data over the instantaneous pressure in the intake manifold, a residual burnt gases rate was calibrated over in order to get better accuracy over in-cylinder mixture mass during closed valve phases in the engine cycle. An example of this calibration is shown in Figure 5 for full load engine tests. Dependency over load and engine speed was then taken into account to create a correlation describing the evolution of this residual burnt gases rate over experimental data, shown in Figure 6. In-cylinder mass could be then determined with this correlation. The error over in-cylinder mass has a major impact on pressure estimation during the compression phase, before start of combustion. This impact is shown in Figure 7.

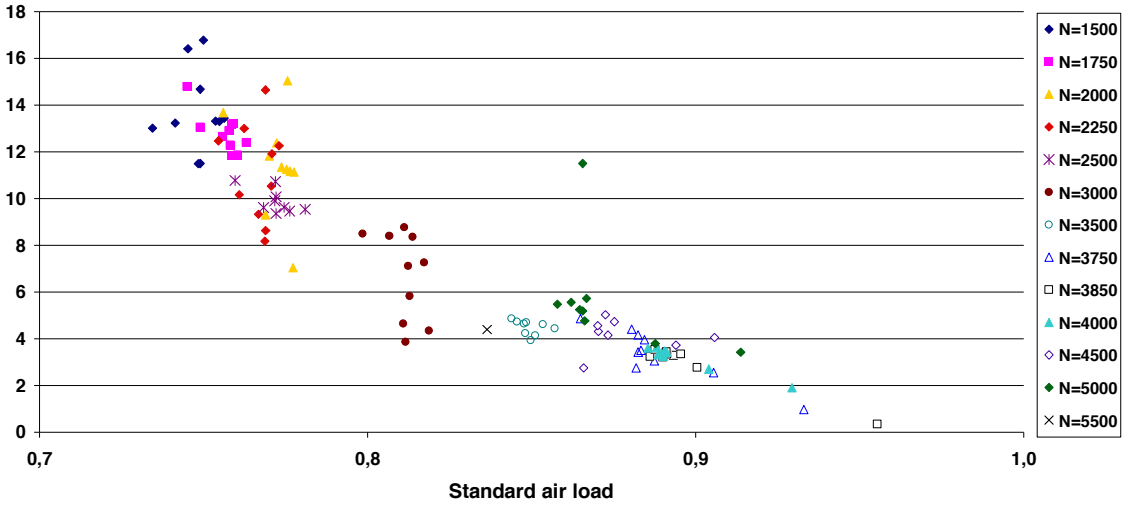

Figure 5: Example of residual gases rate calibration, over full load tests

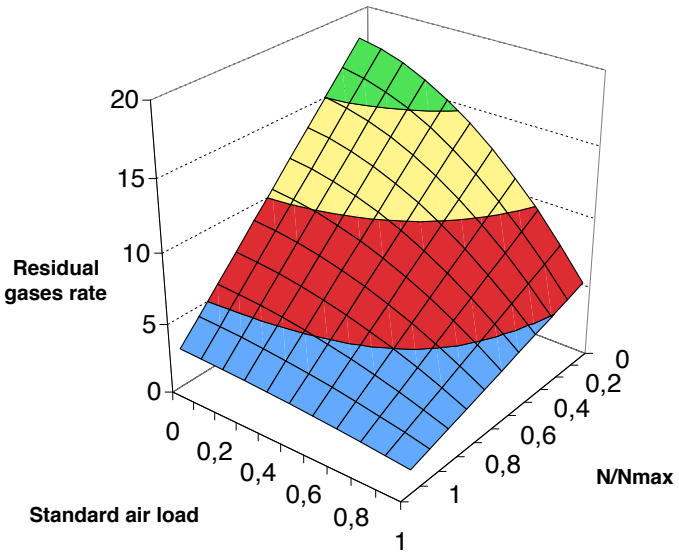

Figure 6: Correlation for residual gases rate as a function of load and engine speed

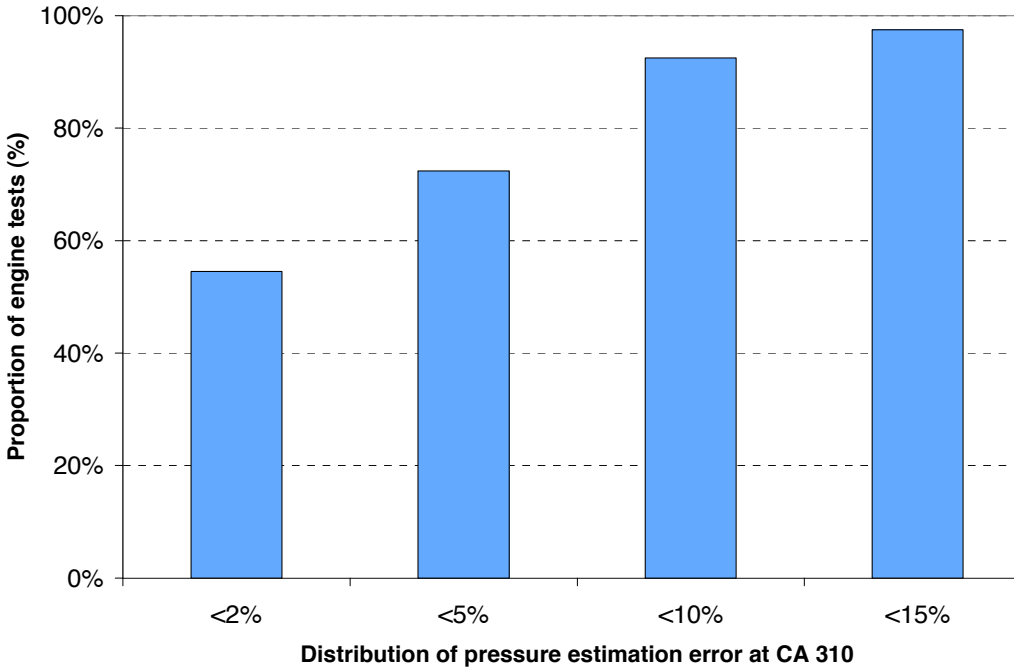

Figure 7: Distribution of pressure estimation error at crank angle 310° over all experimental data while using the correlation for residual gases rate

5.3. Thermal loss and flame initial volume calibrations

Care was then given to the calibration of several CFM-1D parameters: thermal losses and initiation of flame volume at start of combustion. Thermal loss estimation was made with choice of Woschni's correlation [15-16].

$$A = C_1 \cdot V_p + C_2 V_{cyl} \cdot \left(T_1 \frac{P - P_0}{P_1 \cdot V_1} \right)$$

$$h_{conv} = 130 \cdot \frac{PA^{0.8}}{T_{gas}^{0.53}} B^{0.2}$$

$$Q_{losses} = h_{conv} \cdot \left(T_{gas} - T_{wall} \right) \cdot S$$

With:

- V_p : mean velocity of the piston (m/s),
- S : exchange surface (m^2),
- T_{wall} : temperature of the walls (K),
- P, T_{gas} : pressure and temperature of the gases in the combustion chamber (Pa, K),
- B : bore (m),
- V_{cyl} : single cylinder displacement (m^3),
- P_0 : pressure in the chamber if no combustion occurs (Pa),

- P_1, T_1, V_1 : condition in the chamber just before start of combustion.

Two parameters were calibrated: one for the compression phase (C_1) and the other for the expansion phase (C_2), as stated in [16]. They both needed a first rough tumble calibration so as to be able to choose most relevant values for the overall tests. Two constant values were chosen for these two parameters.

The flame initial volume parameter was then calibrated. Various tests showed that choosing a high value for this parameter gives better results for tumble calibration than choosing one too low.

5.4. Tumble calibration

Tumble constant was eventually calibrated with load variation and full load engine tests. The results for tumble parameter obtained for load variation tests are shown in Figure 8. Cylinder pressure evolution has been used for the calculation of the convergence criteria for the tumble constant calibration: Indicated Mean Effective Pressure (IMEP), cycle maximum pressure, crank angle of cycle maximum pressure. Figure 9 shows an example of cylinder pressure simulation with regard to the experimental measures. At this step of model calibration, most of the simulations give satisfactory results with their optimum tumble parameter. Differences can still be observed over the pressure curves as previously described in 5.1.

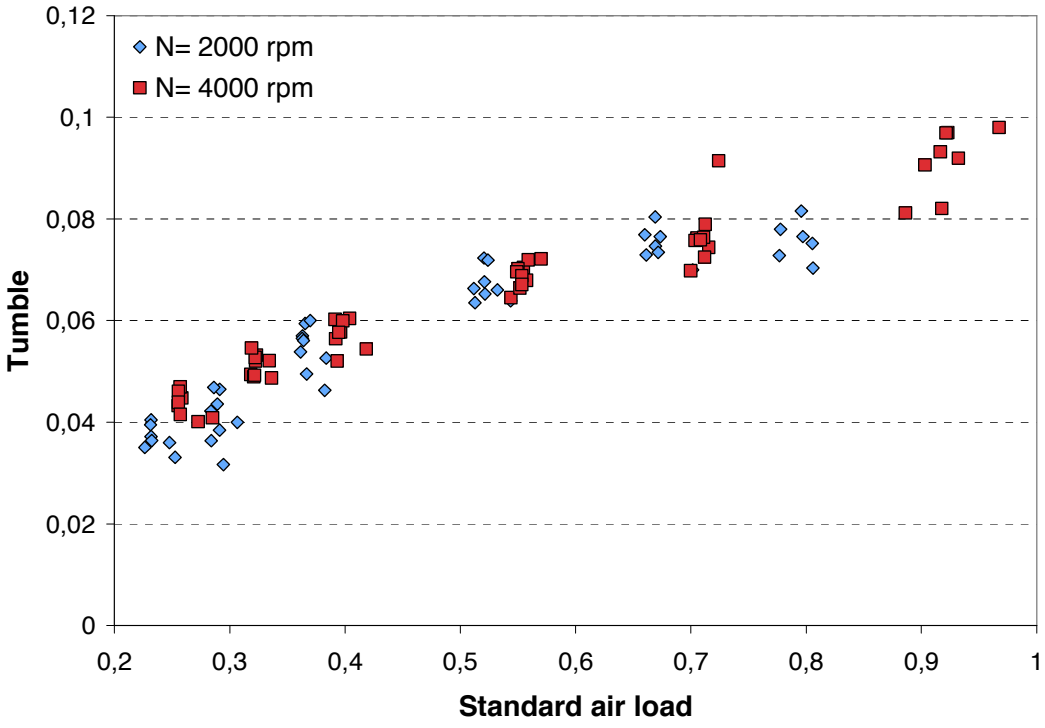

Figure 8: Tumble parameter calibration over load variations engine tests

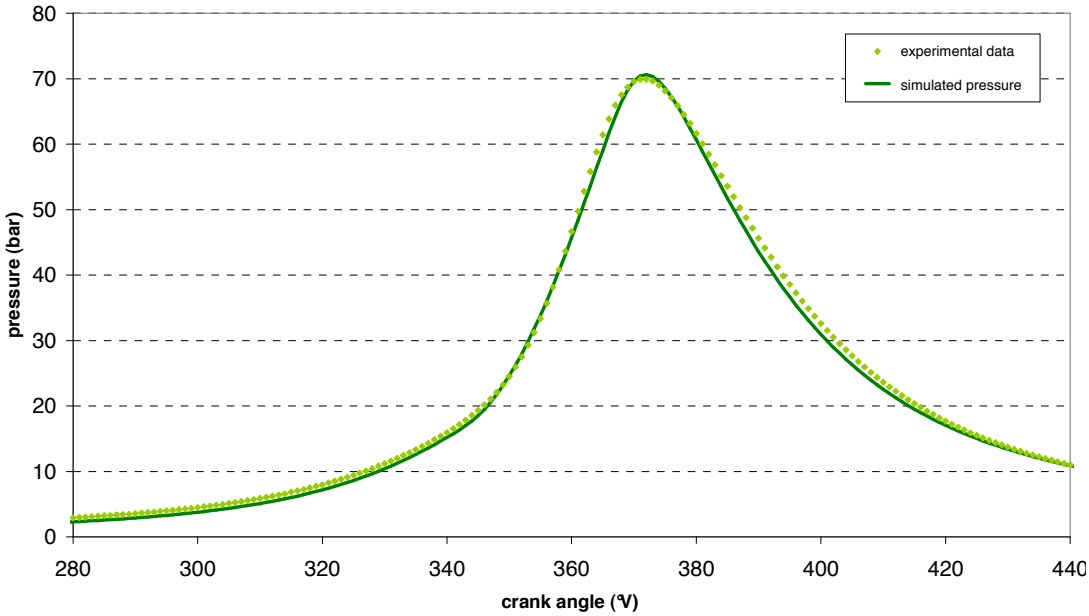

Figure 9: Example of comparison between simulated cylinder pressure and experimental data near top dead center

So as to determine the model's performance over the 80% of experimental data not already used for the calibration, a correlation for the tumble parameter, with respect to load and engine speed, was built with these results of the tumble parameter calibration, as shown in Figure 10. Such a correlation decreases accuracy over the former calibrated points, but enables simulating tendencies outside of these.

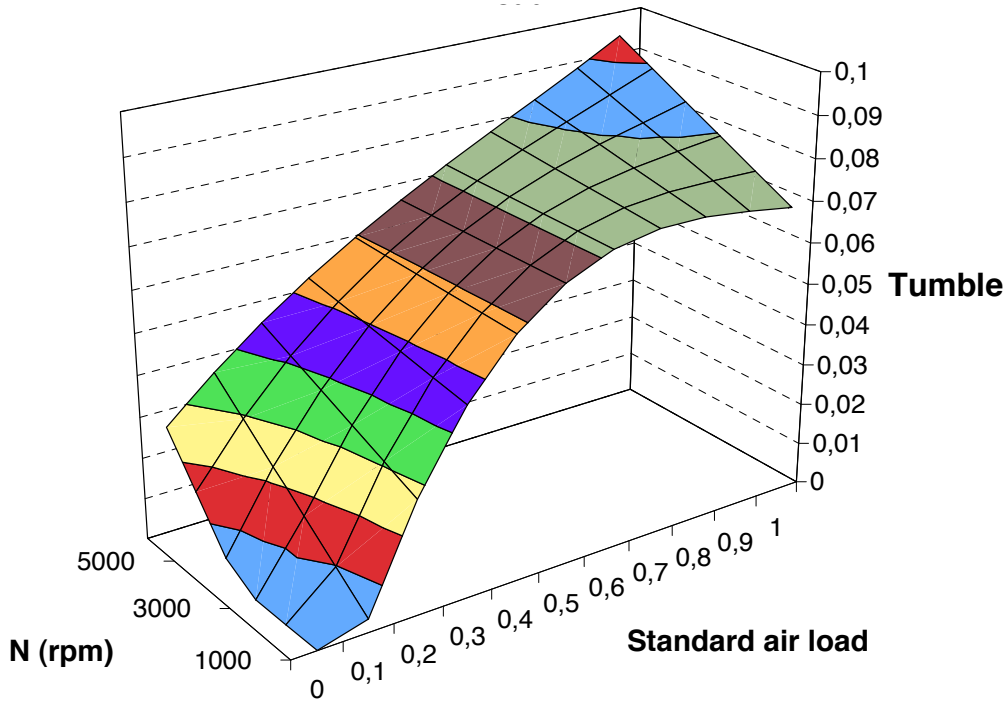

Figure 10: Tumble parameter correlation over engine speed and standard air load

5.5. Results

The resulted calibrated engine model has then been tested over the all range of experimental data. Figure 11, Figure 12 and Figure 13 show the distribution of estimation errors for maximum

cylinder pressure, crank angle of maximum cylinder pressure and IMEP over all the different kinds of engine tests available. Best results are obtained with the points that have been used for calibration. IMEP estimation error remains mainly under 10%. This is quite promising since it is comparable to gasoline model results with calibration of tumble parameter, with no use of the model for realistic wrinkling of flame. Results over maximum peak pressure estimation and phasing are comparable to those obtained on a gasoline engine with IFP-Engine® [17].

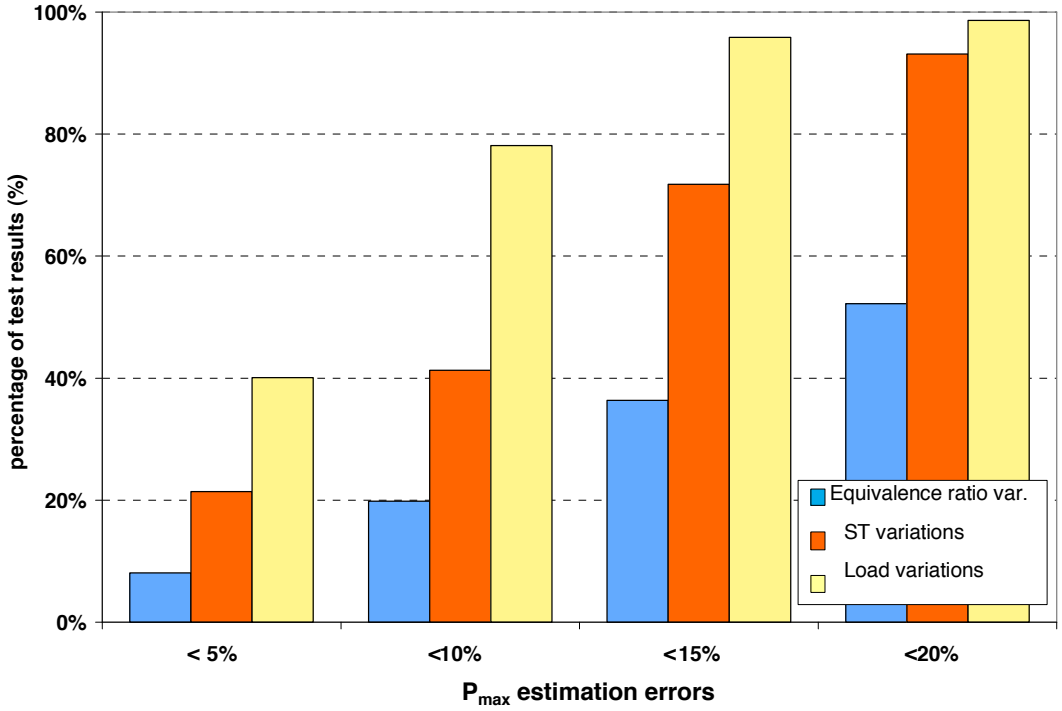

Figure 11: Distribution of maximum cylinder pressure estimation error

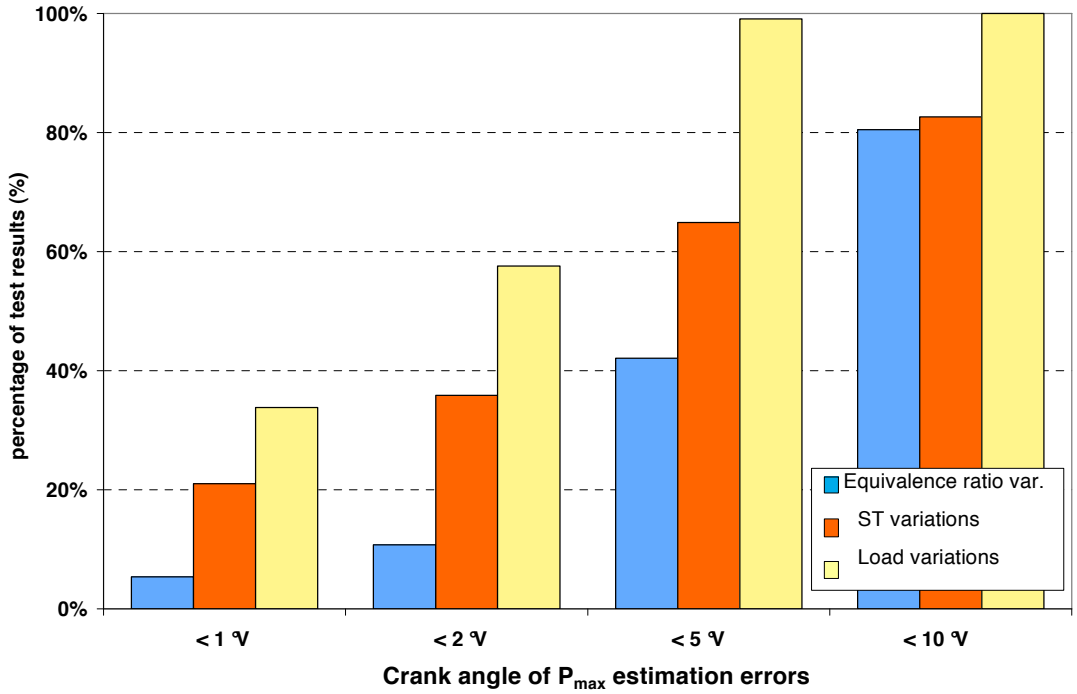

Figure 12: Distribution of crank angle maximum cylinder pressure estimation error

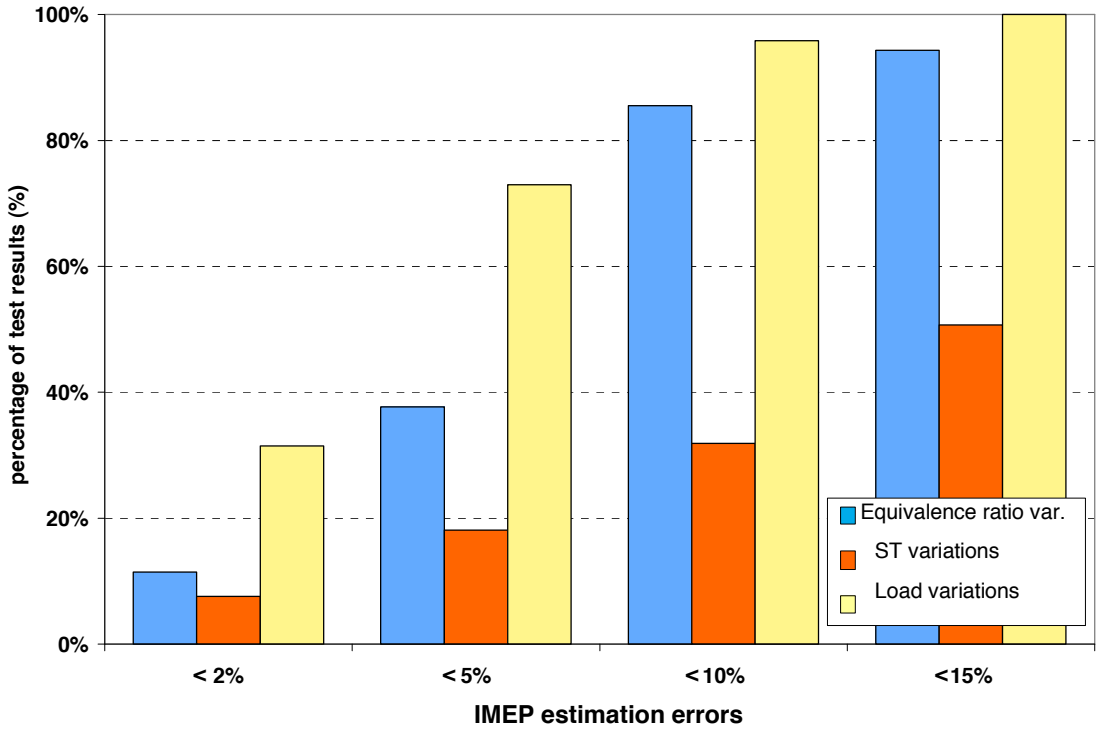

Figure 13: Distribution of IMEP estimation error

Nevertheless, it appears that error over spark timing variation tests and equivalence ratio variations may be triggered by ill-fitted values for C_{dis} and C_{turb} that have been kept to default values in this study. Their influence over turbulent kinetic energy is shown in Figure 14 and Figure 15. If this turbulent kinetic energy phasing along the cycle is not properly done, it triggers non-realistic behavior, while keeping the same operating conditions but with other values for the spark timing.

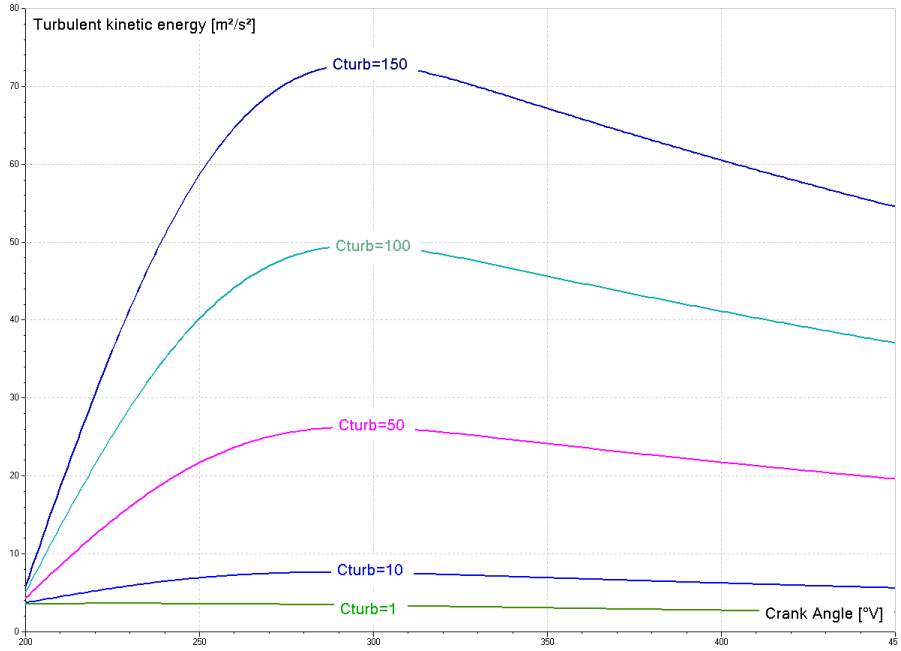

Figure 14: C_{turb} parameter influence on turbulent kinetic energy

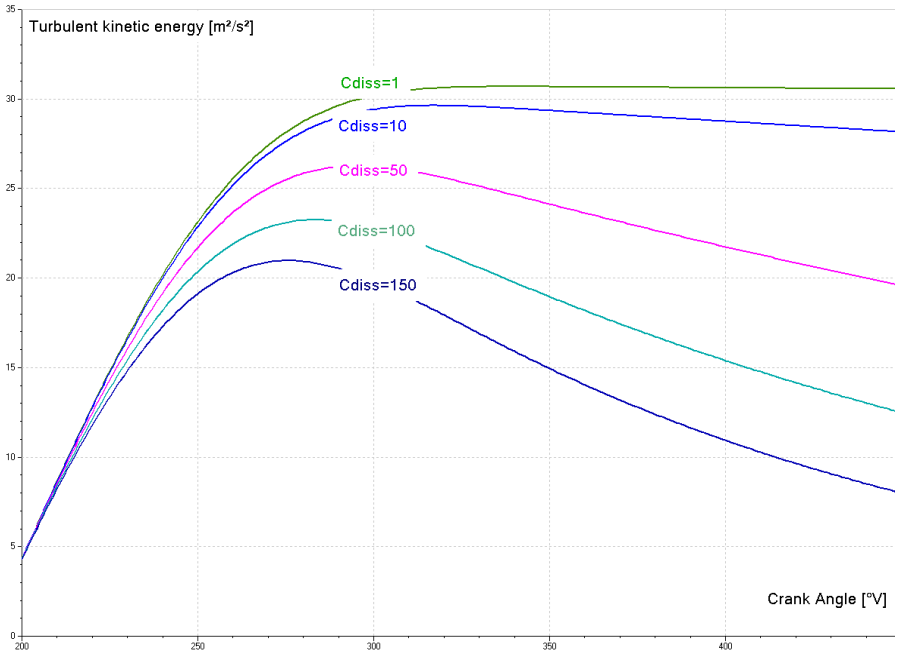

Figure 15: C_{diss} parameter influence on turbulent kinetic energy

Regarding equivalence ratio variation tests, part of the error may be reduced through better calibration of C_{turb} and C_{diss}, since reducing equivalence ratio reduces flame speed and so affects heat release rate and phasing, in a similar way as spark timing variations. If the error remains unsatisfactory, introducing a dependency between flame initial volume parameter and air fuel equivalence ratio will be studied. Since this parameter represents to some extent the radical spread volume at the start of the combustion, it may also be dependent to natural gas quality.

The use of the model for realistic wrinkling of flame will be studied to improve the results. Its enhancing of turbulence description of the early combustion phase may help get better calibrations over IMEP and maximum pressure peak estimation and phasing [17].

a) experimental results

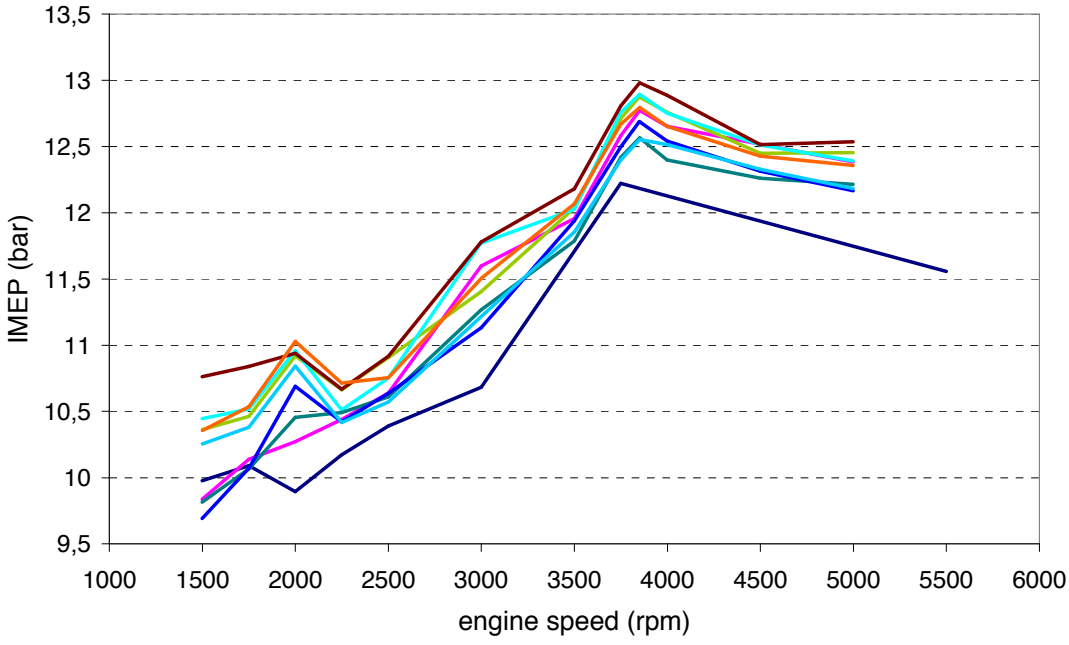

b) simulation

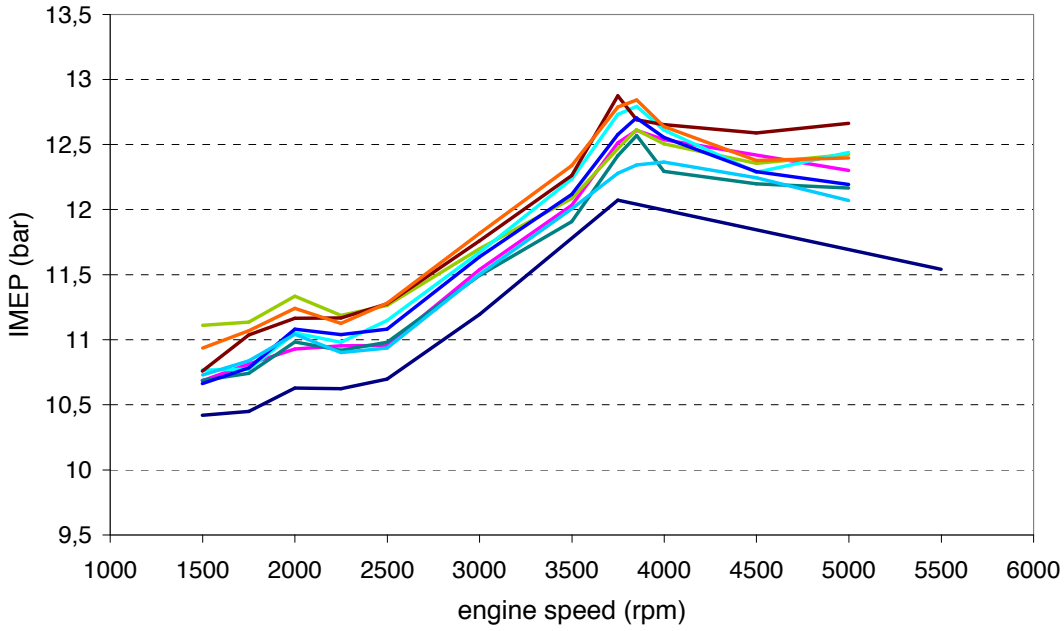

Figure 16: IMEP simulation (a) and experimental (b) results for full load engine operation

The model's satisfactory behavior can be checked through full load curves presented in Figure 16. On the whole, the model gives good orders of magnitude and tendencies. Since the points are not calculated at constant load, it is difficult to highlight whether the model gives accurate tendencies over different natural gas qualities. This ability will be studied with a higher calibration level: introducing wall temperature dependency over load variations, C_{dis} and C_{turb}, model for realistic wrinkling of flame.

Considering the very few parameters calibrated in this first step of the implementation of our homemade model into Imagine.Lab AMESim®, results are quite promising.

6. CONCLUSIONS

These two studies performed by GDF SUEZ increased its expertise in natural gas use as a fuel with:

- the implementation of natural gas issues into an industrial engine simulation tool used by cars and trucks manufacturers,
- the development of a predictive NOx model coupled with a gas engine model.

Both lead to good expectations for following works.

Regarding the NO model that has been implemented with the use of our homemade Fortran 90 engine combustion model, main remarks are the following:

- This first study was focused on NO prediction. Among NOx emissions out of the engine, NO emissions account for a high proportion of these. The same modeling will be done with NO_2 to increase accuracy,
- NO model gives satisfactory error distribution with a quite narrow interval,
- Tendencies in NO formation have been well predicted over the simulated points, with respect to engine speed and gas quality variations,

- As NO production is quite sensitive to temperature level in the burnt gas zone, predictions of NO emissions tendencies over all the simulated points give another confirmation on the relevance of the calculated temperature for burnt gases, and so the whole combustion model used,
- Higher accuracy in the NO prediction may be achieved through thermal loss calibration and introducing a dependency between wall temperature and load variations.

Regarding the implementation of previously studied CNG issues into AMESim® engine simulation tool, main remarks are:

- Satisfactory results with a similar level of accuracy with natural gas operation with the gasoline model prediction abilities over gasoline operations,
- Improving results through calibration of C_{dis} and C_{turb}, model for realistic wrinkling of flame, wall temperature (with dependency over load),

This simulation tool will be then used in industrial research programs with car manufacturer partners, and will help strengthening interactions with car manufacturers and taking better hold on the NGV market development.

7. NOMENCLATURE

C_{dis}: dissipation constant for turbulent kinetic energy calculation,

C_{turb}: turbulence creation constant for turbulent kinetic energy calculation,

IMEP: indicated mean effective pressure (bar),

K_i : reaction kinetic constant of reaction (i) (cm^3/mol.s),

$[X]_e$: concentration at equilibrium of X species (mol/cm^3),

R_i : reaction rate at equilibrium reaction (i) (mol/cm^3.s),

V_p : mean velocity of the piston (m/s),

S : exchange surface (m^2),

T_{wall} : temperature of the walls (K),

P, T_{gas} : pressure and temperature of the gases in the combustion chamber (Pa, K),

B : bore (m),

V_{cyl} : single cylinder displacement (m^3),

P_0 : pressure in the chamber if no combustion occurs (Pa),

P_1, T_1, V_1 : condition in the chamber just before start of combustion.

8. REFERENCES

[1] C. Caillol, G. Berradi, G. Brecq, M. Ramspacher, P. Meunier, A simulation tool for evaluating gas composition effects on engine performance, 2004,

[2] J. B. Heywood, Internal Combustion Engine Fundamentals, McGraw-Hill, New York, 1988,

[3] C. Bowman. Kinetics of pollutant formation and destruction in combustion. Progress in Energy and Combustion Science, 1:33-45, 1975,

[4] J. Miller, C. Bowman. Mechanism and modeling of nitrogen chemistry in combustion. Progress in Energy and Combustion Science, 15:287-338, 1989,

[5] U. Kesgin, « Study on prediction of the effects of design and operating parameters on NOx emissions from a lean-burn natural gas engine », Energy Conversion and Management 44 (2003) 907–921, 2002,

[6] U. Kesgin, « Genetic algorithm and artificial neural network for engine optimization of efficiency and NOx emission », Fuel 83 (2004) 885–895, 2003,

[7] C.D. Rakopoulos, E.G. Giakoumis, D.C. Kyritsis, Validation and sensitivity analysis of a two zone Diesel engine model for combustion and emissions prediction, Energy Conversion and Management 45 (2004) 1471–1495, 2003,

[8] J.A. Caton, Detailled result for nitric oxide emission as determined from a multiple-zone cycle simulation for a spark-ignition engine, ASME-IDES 08-11, 2002,

[9] J.A. Caton, Effects of burn rate parameters on nitric oxide emission for a park ignition engine: Results for a tree-zone, thermodynamic simulation, Department of Mechanical Engineering, Texas A&M University, 2003-01-0720, 2003,

[10] R.S. Fletcher et J.B. Heywood, A model for nitric oxide emission from aircraft gas turbine engine, American Institute of Aeronautics and Astronautics, AIAA Paper n° 71-123, 1971,

[11] W.P.J. Visser et S.C.A. Kluiters, Modeling the effects of operating conditions and alternative fuels on gas turbine performance and emissions, National Aerospace Laboratory NLR, NLR-TP-98629, 1998,

[12] C. Caillol, Influence de la composition du gaz naturel carburant sur la combustion turbulente en limite pauvre dans les moteurs à allumage commandé, PhD thesis, Université de Provence, 2004,

[13] G.F. Hohenberg, Advanced approaches for heat transfer calculations, SAE Paper, (790825), 1979,

[14] Lafossas F.-A., Colin O., Le Berr F., Mennegazzin P., Application of a New 1D Combustion Model to Gasoline Transcient Engine Operation, SAE Paper 2005-01-2107, 2005,

[15] Woschni G., Universally Applicable Equation for the Instantaneous Heat transfer Coefficient in the Internal Combustion Engine, SAE paper 670931, SAE Trans, vol. 76, 1967,

[16] Imagine (LMS), AMESim® V.4.2, Libraries, interfaces and tools, User Manual IFP Engine library, December 2004,

[17] F.-A. Lafossas, S. Richard, Projet PREDIT VECSIM, réunion de clôture du projet VECSIM, Modélisation de la combustion, January 2008,

9. LIST OF TABLES

10. LIST OF FIGURES